ACS OMEGA

Article

Cite This: ACS Omega 2018, 3, 12489−12494

http://pubs.acs.org/journal/acsodf

Titanium Carbide (MXene) as a Current Collector for Lithium-Ion Batteries

Chueh-Han Wang,[†,‡] Narendra Kurra,[†] Mohamed Alhabeb,[†] Jeng-Kuei Chang,[‡,∥] Husam N. Alshareef,[§] and Yury Gogotsi*[,†]

[†]A.J. Drexel Nanomaterials Institute, Department of Materials Science and Engineering, Drexel University, Philadelphia, Pennsylvania 19104, United States

[‡]Institute of Materials Science and Engineering, National Central University, 32001 Taoyuan, Taiwan

[§]Materials Science and Engineering, King Abdullah University of Science and Technology (KAUST), 23955-9600 Thuwal, Kingdom of Saudi Arabia

[∥]Department of Materials Science and Engineering, National Chiao Tung University, 30010 Hsinchu, Taiwan

ABSTRACT: MXenes are a class of two-dimensional (2D) transition-metal carbides and nitrides that are currently at the forefront of 2D materials research. In this study, we demonstrate the use of metallically conductive free-standing films of 2D titanium carbide (MXene) as current-collecting layers (conductivity of ∼8000 S/cm, sheet resistance of 0.5 Ω/sq) for battery electrode materials. Multilayer $Ti_3C_2T_x$ (T_x: surface functional groups −O, −OH, and −F) is used as an anode material and $LiFePO_4$ as a cathode material on 5 μm MXene films. Our results show that the capacities and rate performances of electrode materials using $Ti_3C_2T_x$ MXene current collectors match those of conventional Cu and Al current collectors, but at significantly reduced device weight and thickness. This study opens new avenues for developing MXene-based current collectors for improving volumetric and gravimetric performances of energy-storage devices.

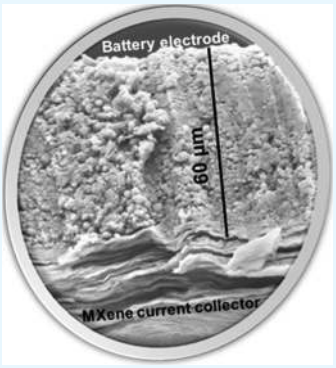

1. INTRODUCTION

Lightweight, flexible, portable electronic devices and wearable gadgets drive demand to develop compact and conformal energy-storage units.[1−3] Li-ion batteries (LIBs) are currently the dominant technology for portable electronics. These batteries are also taking over the electric/hybrid electric vehicles market because of their high energy density and excellent energy efficiency.[4,5] Metal current collectors such as copper (Cu) and aluminum (Al) are typically used as materials for anode and cathode, respectively. However, they do not contribute to capacity, but add up to the total weight and volume, thus reducing the overall energy density of LIB cells significantly. Moreover, the metal surface must be treated to ensure strong adhesion of electrode materials for minimizing the contact resistance and increasing capacity, rate capability, and cycling stability over a pristine metal surface covered with a native oxide layer.[6,7] Importantly, the current collector should not only act as an electrical conductor between the electrode and external circuit but also as a compatible support for coating of electrode materials while being lightweight, mechanically strong, and electrochemically stable.

Traditional metal current collectors are considered to be passive components as they hardly contribute to the overall capacity while accounting for ∼15% (for Al metal collector) and ∼50% (for Cu collector) of total weight of the industrial-scale cathodes and anodes, respectively.[8,9] This limitation has triggered efforts toward developing lightweight current collectors. A variety of carbon-based current collectors including carbon nanotubes,[10−12] carbon paper,[13,14] graphene paper,[15−17] and carbon fiber[18,19] were developed to replace traditional metal foils. For instance, Wang et al. employed current collectors based on superaligned carbon nanotube films, which also showed better wetting, stronger adhesion, and mechanical durability of cast electrode materials.[20] Furthermore, Chen et al. have employed a highly conductive (∼3000 S/cm) reduced graphene oxide film produced by current-induced annealing and demonstrated its applicability as a current collector.[21] However, electrical conductivity is still an issue for those carbon-based current collectors that may need processing at high temperatures to improve their conductivity. Thus, the development of solution-processable two-dimensional (2D) nanomaterials with high electrical conductivity and low sheet resistance through ambient processing is important for fabrication of lightweight current collectors. This is especially true since such devices should be printable, flexible, transparent, and/or attached to a variety of surfaces for sensor networks and Internet of Things applications.

MXenes are a large family of 2D materials, comprising transition-metal carbides, nitrides, and carbonitrides with a general formula, $M_{n+1}X_nT_x$, where M is an early transition

Received: August 14, 2018
Accepted: September 21, 2018
Published: October 3, 2018

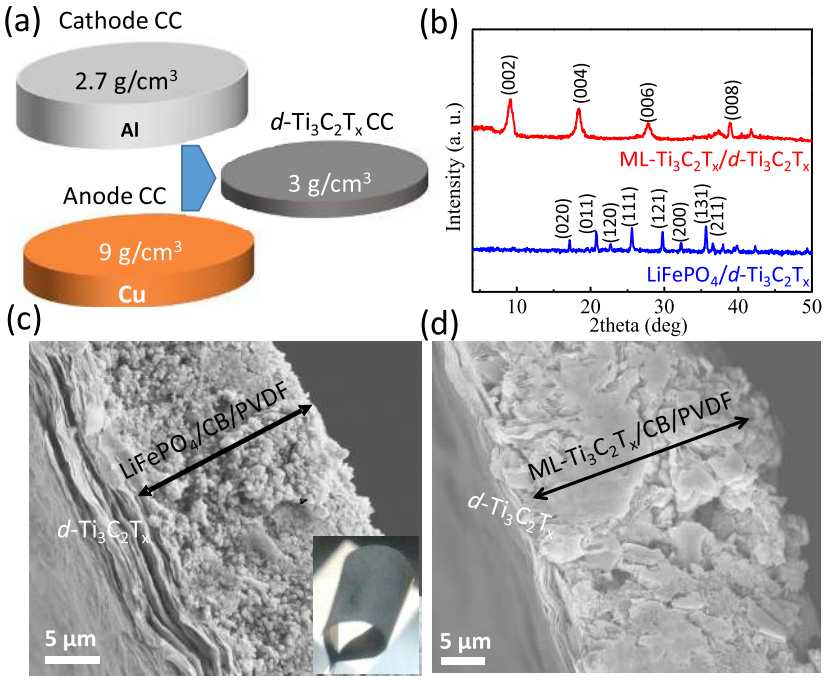

Figure 1. (a) Schematic illustration of Cu and Al foils in comparison with MXene film, where density values are provided. (b) X-ray diffraction (XRD) patterns of LFP and ML-$Ti_3C_2T_x$ cast on d-$Ti_3C_2T_x$. Cross-sectional scanning electron microscopy (SEM) images showing (c) $LiFePO_4$/d-$Ti_3C_2T_x$, the inset shows the digital photograph of the flexible film, and (d) ML-$Ti_3C_2T_x$/d-$Ti_3C_2T_x$ film. CC: current collector; CB: carbon black; PVDF: poly(vinylidene fluoride).

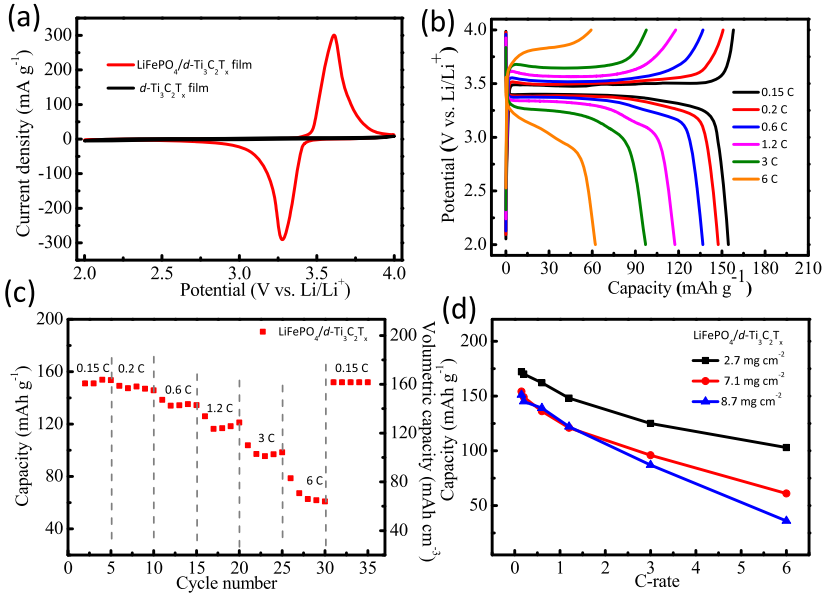

Figure 2. Electrochemical performance of $LiFePO_4$ coated on d-$Ti_3C_2T_x$ film. (a) Cyclic voltammograms of LFP/d-$Ti_3C_2T_x$ and d-$Ti_3C_2T_x$ films at a scan rate of 0.1 mV/s. (b) Charge/discharge profiles of LFP/d-$Ti_3C_2T_x$ at various C-rates, (c) rate performance, and (d) capacity versus C-rates at different mass loadings of 2.7, 7.1, and 8.7 mg/cm^2.

metal, X is a carbon or nitrogen, and T_x stands for various surface terminations (−OH, −O, or −F groups).[22] Because of their compositional versatility and intriguing physicochemical properties, MXenes have shown promise in a variety of applications including electromagnetic interference shielding,[23] wireless communication,[24] and energy storage.[25−32] For instance, titanium carbide (Ti_3C_2) shows electrical conductivity up to 10 000 S/cm[33] and is a 2D hydrophilic metal, obtained through solution processing.[34] Recently, Peng et al. employed large-flake $Ti_3C_2T_x$ as a current collector for demonstrating all-solid-state MXene microsupercapacitors without using metal current collectors.[35] The metallic electrical conductivity, excellent flexibility, and mechanical strength of the delaminated $Ti_3C_2T_x$ (d-$Ti_3C_2T_x$) films prompted us to employ them as current collectors for battery electrodes. Additionally, $Ti_3C_2T_x$ MXene free-standing films have density 3 times lower density compared to that of Cu. These unique

DOI: 10.1021/acsomega.8b02032
ACS Omega 2018, 3, 12489−12494

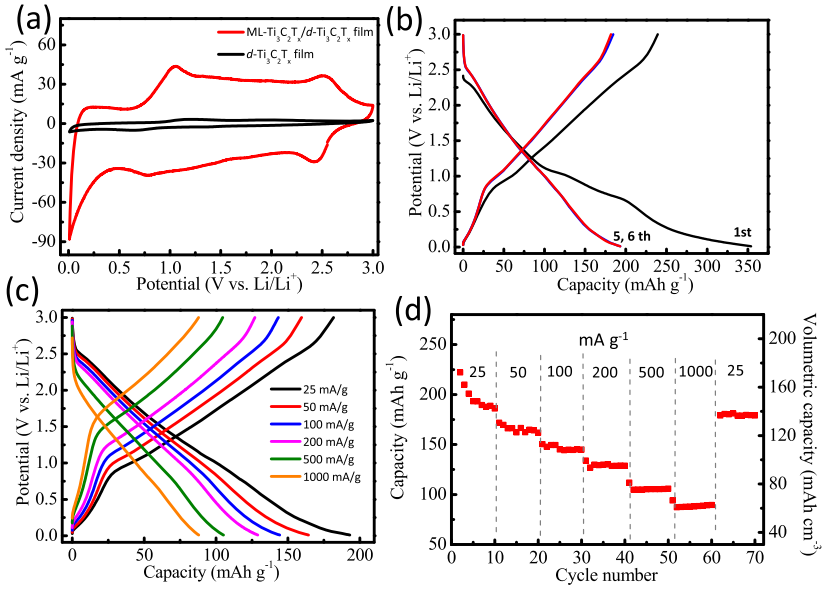

Figure 3. Electrochemical performance of ML-$Ti_3C_2T_x$ coated on d-$Ti_3C_2T_x$ film. (a) Cyclic voltammograms at 0.1 mV/s. (b) Charge−discharge curves for first, fifth, and sixth cycles at a current density of 25 mA/g. (c) Charge−discharge curves at different current densities. (d) Rate performance showing gravimetric and volumetric capacities at varied current densities.

characteristics of titanium carbide MXene free-standing films have hardly been explored.

In this study, we employed a free-standing $Ti_3C_2T_x$ film (~5 μm thickness) as a current collector for casting anode and cathode materials in place of Cu and Al current collectors. To demonstrate the proof of concept, we have used multilayer $Ti_3C_2T_x$ (ML-$Ti_3C_2T_x$) as an anode material and commercial $LiFePO_4$ (LFP) as a cathode material at high mass loadings (2−9 mg/cm^2).

2. RESULTS AND DISCUSSION

$Ti_3C_2T_x$ was shown to exhibit the highest electrical conductivity in the MXene family and among other solution-processable 2D nanomaterials. Additionally, we found that thickness of MXene film less than 5 μm is sufficient for both electrical conduction and mechanical support[36] for typical mass loadings of electrode materials in the range of 2−9 mg/cm^2. The delaminated $Ti_3C_2T_x$ (d-$Ti_3C_2T_x$) films (1−5 μm thick) were made by vacuum-assisted filtration and had a packing density of ~3 g/cm^3. This shows that the thin layers of MXene may have an advantage over LIB current collectors, including Al (thickness = 20 μm, density = 2.7 g/cm^3) and Cu foils (thickness = 12 μm, density = 9 g/cm^3).[1] The schematic shown in Figure 1a illustrates the comparison between d-$Ti_3C_2T_x$ free-standing films and traditional Al and Cu metal current collectors. The density of d-$Ti_3C_2T_x$ is similar to that of Al, while it is 3 times lower compared to that of Cu. This is an advantage of using $Ti_3C_2T_x$ MXene current collector for reducing the total volume and weight of LIB electrodes by at least 3 times.

The XRD patterns of multilayer $Ti_3C_2T_x$ (ML-$Ti_3C_2T_x$) and $LiFePO_4$ cast on d-$Ti_3C_2T_x$ film are shown in Figure 1b. The *d*-spacing of ML-$Ti_3C_2T_x$ was found to be 9.6 Å. $LiFePO_4$ XRD pattern is in good agreement with the literature reports. Figure 1c,d shows cross-sectional images of $LiFePO_4$/d-$Ti_3C_2T_x$ and ML-$Ti_3C_2T_x$/d-$Ti_3C_2T_x$ electrodes, respectively. As shown in the SEM images, the interface between d-$Ti_3C_2T_x$ film and coated layer was uniform without voids or deformation, confirming the good connection between d-$Ti_3C_2T_x$ film and electrode materials. The highly flexible nature of the cast electrode on d-$Ti_3C_2T_x$ film can be demonstrated through bending the entire stack to extreme angles, up to 180°, as shown in the inset of Figure 1c. We have not observed any crack formation after bending the electrode for repeated bending cycles, indicating the mechanical integrity of the entire electrode stack (60 μm) on d-$Ti_3C_2T_x$ film. The optimal thickness of electrode materials (for single side coating) is found to be 10 times that of MXene film thickness.

The electrochemical performance of $LiFePO_4$/d-$Ti_3C_2T_x$ film was studied at different mass loadings (Figure 2). The cyclic voltammograms of $LiFePO_4$/d-$Ti_3C_2T_x$ and bare d-$Ti_3C_2T_x$ electrodes were compared at a scan rate of 0.1 mV/s, as shown in Figure 2a. Distinctive sharp oxidation and reduction peaks were observed at 3.61 and 3.27 V (vs Li/Li$^+$), corresponding to Li$^+$ extraction and insertion in the $LiFePO_4$ structure (Fe^{2+}/Fe^{3+}), respectively. In contrast, bare d-$Ti_3C_2T_x$ film showed very low current response in the cyclic voltammetry (CV) scan, indicating the electrochemical stability of the compact d-$Ti_3C_2T_x$ film. Since the mass loading of active layer is >3 mg/cm^2, we have not noticed any parasitic reactions due to interaction of electrolyte with the functional groups on MXene sheets. At such high mass loadings, MXene serves only as a passive current collector as it is coated densely by the electrode materials.

Figure 2b shows charge/discharge profiles of $LiFePO_4$ (7.1 mg/cm^2) measured in the range of 0.15C−6C rates, and the corresponding discharge capacities were estimated to be 155, 147, 137, 117, 97, and 62 mAh/g. As shown in Figure 2c, when the C-rate is increased from 0.15 to 6C, the electrode retains 40% of its initial capacity, which means that the conductivity of d-$Ti_3C_2T_x$ film is sufficient for characterizing the electrochemical performance of $LiFePO_4$ electrodes at a thickness of 60 μm. After reverting to 0.15C rate, the capacity rebounded to its initial values (155 mAh/g and 165 mAh/cm^3) and remained stable, confirming the reversibility and suggesting that no degradation occurred during high-rate cycling of

DOI: 10.1021/acsomega.8b02032
ACS Omega 2018, 3, 12489−12494

$LiFePO_4$/d-$Ti_3C_2T_x$ electrodes. Figure 2d shows the capacity versus C-rate measured for different $LiFePO_4$ loadings (2.7, 7.1, and 8.7 mg/cm^2) on d-$Ti_3C_2T_x$ film. Even at a mass loading of 8.7 mg/cm^2, LFP electrode showed a capacity of 122 mAh/g at 1.2 C rate, which matches with the literature reports employing traditional Al current collectors at similar mass loadings of electrode materials.[37]

$Ti_3C_2T_x$ MXene has been explored for electrochemical storage because of its layered morphology with electrochemically active surfaces available for metal-ion storage.[27−30,38,39] Electrochemical performance of ML-$Ti_3C_2T_x$/d-$Ti_3C_2T_x$ is shown in Figure 3. Figure 3a compares the CV profiles of ML-$Ti_3C_2T_x$/d-$Ti_3C_2T_x$ electrode and bare d-$Ti_3C_2T_x$ film at a scan rate of 0.1 mV/s. As shown in the CV curves, the capacity of bare d-$Ti_3C_2T_x$ film is much smaller than that of ML-$Ti_3C_2T_x$/d-$Ti_3C_2T_x$ electrode, meaning that the major capacity contribution is from the top ML-$Ti_3C_2T_x$. The typical areal mass loading of ML-$Ti_3C_2T_x$ is ∼3.9 mg/cm^2. Sloping charge/discharge profiles are typical of MXenes electrodes, as shown in Figure 3b,c. ML-$Ti_3C_2T_x$/d-$Ti_3C_2T_x$ electrode showed first-cycle Coulombic efficiency of 67% at a current density of 25 mA/g and stabilized capacity of 180 mAh/g after fifth cycle. When current density was increased to 1 A/g, the capacity decreased to 87 mAh/g with 48% capacity retention (Figure 3d). The capacity also rebounded to the initial value of 180 mAh/g (Figure 3d) by reverting current density to 25 mA/g, indicating good rate capability and reversibility of ML-$Ti_3C_2T_x$/d-$Ti_3C_2T_x$ electrode.

The realized capacity of the electrodes was calculated by considering the total weight (estimated on the basis of density of the current collectors but not relying on the absolute thickness values), including current collector and active material stack used for testing half-cell measurements. There is not much gain using MXene current collector instead of Al because of same values of density in both cases (at the same thickness level). As shown in Figure 4, the gravimetric capacity

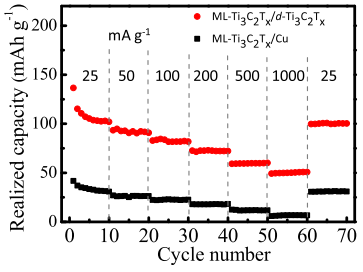

Figure 4. Realized capacity (based on the total weight of active materials and the current collector) of ML-$Ti_3C_2T_x$ (on a Cu foil) and ML-$Ti_3C_2T_x$ (on d-$Ti_3C_2T_x$ film) electrodes at different current densities.

obtained using d-$Ti_3C_2T_x$ film is 3 times higher than using a Cu foil as a current collector. This is clearly an advantage for using highly conductive MXene films, which can effectively reduce the total weight of the anode stack of LIB. This study is a demonstration of the concept of using MXene current collectors; however, future studies should focus on the influence of the surface functionality of MXenes on the contact impedance using systematic electrochemical impedance spectroscopy investigations and further improvements through surface modifications.

Although this study demonstrated the feasibility of MXene thin films as current collectors in small devices, the thermal characteristics of MXene films should be studied to ensure efficient heat dissipation during battery cycling. Heat produced during charging/discharging of battery electrodes in large-size batteries can be dissipated easily if the current collector has a high thermal conductivity. Tensile strength of MXene current collectors should also be investigated to ensure that winding of electrodes is possible. However, the available data on single-layer MXene flakes[40] and films[41] suggest that the required mechanical strength can be achieved. However, there is no published information about thermal conductivity of Ti_3C_2 films. Future investigations should focus on these issues to validate the viability of MXene films as current collectors in a variety of batteries.

3. CONCLUSIONS

We demonstrated application of a highly conductive thin d-$Ti_3C_2T_x$ current collector for cathode and anode electrode materials instead of traditional metal collectors. $Ti_3C_2T_x$ film showed compatibility with coatings of $LiFePO_4$ and ML-$Ti_3C_2T_x$ electrodes without additional surface treatments. Compared to Cu metal foil, d-$Ti_3C_2T_x$ film offered reduced cell weight and improved volumetric capacity for anode electrode stack. Our results suggest that MXene current collector could be a potential candidate for developing flexible and lightweight energy-storage devices.

4. EXPERIMENTAL SECTION

4.1. Fabrication of $Ti_3C_2T_x$ Films. All chemicals were used as received without further purification. Layered ternary carbide Ti_3AlC_2 (MAX phase) powder (particle size <40 μm) was obtained from Carbon-Ukraine, Ltd. $Ti_3C_2T_x$ MXene was synthesized following the minimal intensive layer delamination method by selective etching of aluminum from Ti_3AlC_2 using in situ hydrofluoric acid (HF)-forming etchant, as previously reported elsewhere.[34] Herein, 1 g of Ti_3AlC_2 powder was slowly added into a solution of 1 g of lithium fluoride (LiF, Alfa Aesar, >98%) in 20 mL of 9 M hydrochloric acid (HCl, Fisher, technical grade, 35−38%) and stirred for 24 h at 35 °C. The acidic suspension was washed with deionized (DI) water until pH ≥ 6 via centrifugation at 3500 rpm (5 min per cycle) and decantation of the supernatant after each cycle. Around pH ≥ 6, a stable dark-green supernatant of $Ti_3C_2T_x$ was observed and then collected after 30 min centrifugation at 3500 rpm. The resulting delaminated $Ti_3C_2T_x$ (d-$Ti_3C_2T_x$) was filtered and dried under vacuum at 70 °C overnight to obtain free-standing films.

4.2. Synthesis of Multilayer $Ti_3C_2T_x$. The etching solution was prepared by adding 1 mL of concentrated HF to 9 mL of H_2O to produce 5 wt % HF, which was used for etching 1 g of Ti_3AlC_2 powder. While stirring at 400 rpm, Ti_3AlC_2 powder was slowly added to the etchants and the temperature of the bath was raised to 40 °C after the complete addition of MAX powder and the reaction was continued for 15 h. Furthermore, washing was done with DI water via centrifugation for 5 min at 3500 rpm several times. The colorless acidic supernatant was decanted after each wash until reaching pH ≥ 6. After this stage, the product was collected via vacuum filtration over a filter membrane with pore size less than 0.45 μm. Then, the obtained powder sample was dried at 200 °C under vacuum for 12 h.

DOI: 10.1021/acsomega.8b02032
ACS Omega 2018, 3, 12489−12494

4.3. Materials Characterization. X-ray diffraction (XRD) analysis of ML-$Ti_3C_2T_x$, and $LiFePO_4$ (MTI Corp., product #EQ-Lib-LFPOKJ2) was performed on a Rigaku Smart Lab (Tokyo, Japan) diffractometer using Cu Kα radiation, λ = 1.5406 Å. Voltage and current settings were 40 kV and 44 mA, respectively, with a step scan of 0.04°, 2θ range 5−50°, and dwell time of 0.5 s. The cross sections of the samples were imaged using a scanning electron microscope (SEM) (Zeiss Supra 50VP, Germany). The electrical conductivity of the samples was measured using a four-point probe (ResTest v1, Jandel Engineering Ltd., Bedfordshire, U.K.) with a probe distance of 1 mm.

4.4. Coin Cell Assembly and Electrochemical Analysis. $LiFePO_4$ (MTI Corp., product #EQ-Lib-LFPOKJ2) and ML-$Ti_3C_2T_x$ were used as active materials to cast on d-$Ti_3C_2T_x$ films. The electrodes were prepared by mixing active materials (80 wt %), carbon black (10 wt %), and poly(vinylidene difluoride) binder (10 wt %) in *N*-methylpyrrolidone to make a slurry separately. After mixing, a uniform slurry was coated on d-$Ti_3C_2T_x$ film and dried under vacuum at 70 °C for 12 h. For comparison, $LiFePO_4$ and $Ti_3C_2T_x$ slurries were coated on Al and Cu foils, respectively, using the same procedure mentioned above.

After drying, electrodes were roll-pressed and punched to match the required dimensions of CR2032 coin cell. A lithium foil was used as the reference and counter electrode for half-cell measurements. Celgard polypropylene membrane was used as a separator between working electrodes and Li metal. 1 M $LiPF_6$ dissolved in ethylene carbonate and diethyl carbonate with a volume ratio of 1:1 was used as the electrolyte. The CR2032 coin cells were assembled in an argon-filled glovebox (VT, Vacuum Technologies) with moisture and oxygen levels less than 0.1 ppm. Charge−discharge measurements were performed at different current densities in the potential windows matching the chosen electrode system using an Arbin battery tester (Arbin BT-2143-11U, College Station, TX). Cyclic voltammetry (CV) was conducted using VMP3 (BioLogic, France) between 0.01 and 3.0 V versus Li/Li^+ at a scan rate of 0.1 mV/s.

AUTHOR INFORMATION

Corresponding Author

*E-mail: gogotsi@drexel.edu.

ORCID

Mohamed Alhabeb: 0000-0002-9460-8548
Jeng-Kuei Chang: 0000-0002-8359-5817
Husam N. Alshareef: 0000-0001-5029-2142
Yury Gogotsi: 0000-0001-9423-4032

Notes

The authors declare no competing financial interest.

ACKNOWLEDGMENTS

C.-H.W. was supported by the Ministry of Science and Technology of Taiwan under Grant No. 105-2917-I-008-008. Research reported in this publication was supported by King Abdullah University of Science and Technology (KAUST) under the KAUST-Drexel Competitive Research Grant (URF/1/2963-01-01). We thank Evan Quain for helpful comments on this article.

REFERENCES

(1) Wang, X.; Lu, X.; Liu, B.; Chen, D.; Tong, Y.; Shen, G. Flexible energy-storage devices: Design consideration and recent progress. *Adv. Mater.* **2014**, *26*, 4763−4782.

(2) Li, L.; Wu, Z.; Yuan, S.; Zhang, X.-B. Advances and Challenges for flexible energy storage and conversion devices and systems. *Energy Environ. Sci.* **2014**, *7*, 2101−2122.

(3) Yousaf, M.; Shi, H. T. H.; Wang, Y.; Chen, Y.; Ma, Z.; Cao, A.; Naguib, H. E.; Han, R. P. S. Novel pliable electrodes for flexible electrochemical energy storage devices: recent progress and challenges. *Adv. Energy Mater.* **2016**, *6*, No. 1600490.

(4) Tarascon, J.-M.; Armand, M. Issues and challenges facing rechargeable lithium batteries. *Nature* **2001**, *414*, 359−367.

(5) Goodenough, J. B.; Kim, Y. Challenges for rechargeable Li batteries. *Chem. Mater.* **2010**, *22*, 587−603.

(6) Liu, W.; Song, M.-S.; Kong, B.; Cui, Y. Flexible and stretchable energy storage: recent advances and future perspectives. *Adv. Mater.* **2017**, *29*, No. 160343.

(7) Foreman, E.; Zakri, W.; Sanatimoghaddam, M. H.; Modjtahedi, A.; Pathak, S.; Kashkooli, A. G.; Garafolo, N. G.; Farhad, S. A review of inactive materials and components of flexible lithium-ion batteries. *Adv. Sustainable Syst.* **2017**, *1*, No. 1700061.

(8) Johnson, B. A.; White, R. E. Characterization of commercially available lithium-ion batteries. *J. Power Sources* **1998**, *70*, 48−54.

(9) Zhou, G.; Li, F.; Cheng, H.-M. Progress in flexible lithium batteries and future prospects. *Energy Environ. Sci.* **2014**, *7*, 1307−1338.

(10) Hu, J. W.; Wu, Z. P.; Zhong, S. W.; Zhong, W. B.; Suresh, S.; Metha, A.; Koratkar, N. Folding insensitive, high energy density lithium-ion battery featuring carbon nanotube current collectors. *Carbon* **2015**, *87*, 292−298.

(11) Cui, L.-F.; Hu, L.; Choi, J. W.; Cui, Y. Light-weight free-standing carbon nanotube-silicon films for anodes of lithium ion batteries. *ACS Nano* **2010**, *4*, 3671−3678.

(12) Lee, S. W.; Gallant, B. M.; Lee, Y.; Yoshida, N.; Kim, D. Y.; Yamada, Y.; Noda, S.; Yamada, A.; Shao-Horn, Y. Self-standing positive electrodes of oxidized few-walled carbon nanotubes for light-weight and high-power lithium batteries. *Energy Environ. Sci.* **2012**, *5*, 5437−5444.

(13) Arbizzani, C.; Lazzari, M.; Mastragostino, M. Lithiation/delithiation performance of Cu_6Sn_5 with carbon paper as current collector. *J. Electrochem. Soc.* **2005**, *152*, A289−A294.

(14) Yan, J.; Liu, X.; Qi, H.; Li, W.; Zhou, Y.; Yao, M.; Li, B. High-performance lithium-sulfur batteries with a cost-effective carbon paper electrode and high sulfur-loading. *Chem. Mater.* **2015**, *27*, 6394−6401.

(15) Rana, K.; Singh, J.; Lee, J.-T.; Park, J. H.; Ahn, J.-H. Highly conductive freestanding graphene films as anode current collectors for flexible lithium-ion batteries. *ACS Appl. Mater. Interfaces* **2014**, *6*, 11158−11166.

(16) Gwon, H.; Kim, H.-S.; Lee, K. U.; Seo, D.-H.; Park, Y. C.; Lee, Y.-S.; Ahn, B. T.; Kang, K. Flexible energy storage devices based on graphene paper. *Energy Environ. Sci.* **2011**, *4*, 1277−1283.

(17) Li, N.; Chen, Z.; Ren, W.; Li, F.; Cheng, H.-M. Flexible Graphene-based lithium ion batteries with ultrafast charge and discharge rates. *Proc. Natl. Acad. Sci. U.S.A.* **2012**, *109*, 17360−17365.

(18) Guo, J.; Sun, A.; Wang, C. A Porous silicon-carbon anode with high overall capacity on carbon fiber current collector. *Electrochem. Commun.* **2010**, *12*, 981−984.

(19) Martha, S. K.; Kiggans, J. O.; Nanda, J.; Dudney, N. J. Advanced lithium battery cathodes using dispersed carbon fibers as the current collector batteries and energy storage. *J. Electrochem. Soc.* **2011**, *158*, A1060−A1066.

(20) Wang, K.; Luo, S.; Wu, Y.; He, X.; Zhao, F.; Wang, J.; Jiang, K.; Fan, S. Super-aligned carbon nanotube films as current collectors for lightweight and flexible lithium ion batteries. *Adv. Funct. Mater.* **2013**, *23*, 846−853.

(21) Chen, Y.; Fu, K.; Zhu, S.; Luo, W.; Wang, Y.; Li, Y.; Hitz, E. M.; Yao, Y.; Dai, J.; Wan, J.; Danner, V. A.; Li, T.; Hu, L. Reduced

DOI: 10.1021/acsomega.8b02032
ACS Omega 2018, 3, 12489−12494

graphene oxide films with ultra-high conductivity as Li-ion battery current collectors. *Nano Lett.* **2016**, *16*, 3616−3623.
(22) Anasori, B.; Lukatskaya, M. R.; Gogotsi, Y. 2D metal carbides and nitrides (MXenes) for energy storage. *Nat. Rev. Mater.* **2017**, *2*, No. 16098.
(23) Shahzad, F.; Alhabeb, M.; Hatter, B. C.; Anasori, B.; Hong, S. M.; Koo, C. M.; Gogotsi, Y. Electromagnetic interference shielding with 2D transition metal carbides (MXenes). *Science* **2016**, *353*, 1137−1140.
(24) Sarycheva, A.; Polemi, A.; Liu, Y.; Dandekar, K.; Anasori, B.; Gogotsi, Y. 2D titanium carbide (MXene) for wireless communication. *Sci. Adv.* **2018**, *4*, No. eaau0920.
(25) Xia, Y.; Mathis, T. S.; Zhao, M.-Q.; Anasori, B.; Dang, A.; Zhou, Z.; Cho, H.; Gogotsi, Y.; Yang, S. Thickness-independent capacitance of vertically aligned liquid-crystalline MXenes. *Nature* **2018**, *557*, 409−412.
(26) Lukatskaya, M. R.; Mashtalir, O.; Ren, E. C.; Dall'Agnese, Y.; Rozier, P.; Taberna, P. L.; Naguib, M.; Simon, P.; Barsoum, M. W.; Gogotsi, Y. Cation intercalation and high volumetric capacitance of two-dimensional titanium carbide. *Science* **2013**, *341*, 1502−1505.
(27) Wang, X.; Kajiyama, S.; Iinuma, H.; Hosono, E.; Oro, S.; Moriguchi, I.; Okubo, M.; Yamada, A. Pseudocapacitance of MXene nanosheets for high-power sodium-ion hybrid capacitors. *Nat. Commun.* **2015**, *6*, No. 6544.
(28) Kajiyama, S.; Szabova, L.; Sodeyama, K.; Iinuma, H.; Morita, R.; Gotoh, K.; Tateyama, Y.; Okubo, M.; Yamada, A. Sodium-ion intercalation mechanism in MXene nanosheets. *ACS Nano* **2016**, *10*, 3334−3341.
(29) VahidMohammadi, A.; Hadjikhani, A.; Shahbazmohamadi, S.; Beidaghi, M. Two-dimensional vanadium carbide (MXene) as a high-capacity cathode material for rechargeable aluminum batteries. *ACS Nano* **2017**, *11*, 11135−11144.
(30) Jiang, Q.; Kurra, N.; Alhabeb, M.; Gogotsi, Y.; Alshareef, H. N. All pseudocapacitive MXene-RuO_2 asymmetric supercapacitors. *Adv. Energy Mater.* **2018**, *8*, No. 1703043.
(31) Yu, L.; Hu, L.; Anasori, B.; Liu, Y.-T.; Zhu, Q.; Zhang, P.; Gogotsi, Y.; Xu, B. MXene-bonded activated carbon as a flexible electrode for high-performance supercapacitors. *ACS Energy Lett.* **2018**, *3*, 1597−1603.
(32) Liu, Y.-T.; Zhang, P.; Sun, N.; Anasori, B.; Zhu, Q.-Z.; Liu, H.; Gogotsi, Y.; Xu, B. Self-assembly of transition metal oxide nanostructures on MXene nanosheets for fast and stable lithium storage. *Adv. Mater.* **2018**, *30*, No. 1707334.
(33) Zhang, C. J.; Anasori, B.; Seral-Ascaso, A.; Park, S.-H.; McEvoy, E.; Shmeliov, A.; Duesberg, G. S.; Coleman, J. N.; Gogotsi, Y.; Nicolosi, V. Transparent, flexible, and conductive 2D titanium carbide (MXene) films with high volumetric capacitance. *Adv. Mater.* **2017**, *29*, No. 1702678.
(34) Alhabeb, M.; Maleski, K.; Anasori, B.; Lelyukh, P.; Clark, L.; Sin, S.; Gogotsi, Y. Guidelines for synthesis and processing of two-dimensional titanium carbide ($Ti_3C_2T_x$ MXene). *Chem. Mater.* **2017**, *29*, 7633−7644.
(35) Peng, Y. Y.; Akuzum, B.; Kurra, N.; Zhao, M.-Q.; Alhabeb, M.; Anasori, B.; Kumbur, E. C.; Alshareef, H. N.; Ger, M.-D.; Gogotsi, Y. All-MXene (2D titanium carbide) solid-state microsupercapacitors for on-chip energy storage. *Energy Environ. Sci.* **2016**, *9*, 2847−2854.
(36) Kurra, N.; Alhabeb, M.; Maleski, K.; Wang, C.-H.; Alshareef, H.; Gogotsi, Y. Bistacked titanium carbide (MXene) anodes for hybrid sodium ion capacitors. *ACS Energy Lett.* **2018**, *3*, 2094−2100.
(37) Nitta, N.; Wu, F.; Lee, J. T.; Yushin, G. Li-ion battery materials: present and future. *Mater. Today* **2015**, *18*, 252−264.
(38) Kajiyama, S.; Szabova, L.; Iinuma, H.; Sugahara, A.; Gotoh, K.; Sodeyama, K.; Tateyama, Y.; Okubo, M.; Yamada, A. Enhanced Li-ion accessibility in MXene titanium carbide by steric chloride termination. *Adv. Energy Mater.* **2017**, *7*, No. 1601873.
(39) Yu, P.; Cao, G.; Yi, S.; Zhang, X.; Li, C.; Sun, X.; Wang, K.; Ma, Y. Binder-free 2D titanium carbide (MXene)/carbon nanotube composites for high-performance lithium-ion capacitors. *Nanoscale* **2018**, *10*, 5906−5913.
(40) Lipatov, A.; Lu, H.; Alhabeb, M.; Anasori, B.; Gruverman, A.; Gogotsi, Y.; Sinitskii, A. Elastic properties of 2D $Ti_3C_2T_x$ MXene monolayers and bilayers. *Sci. Adv.* **2018**, *4*, No. eaat0491.
(41) Ling, Z.; Ren, C. E.; Zhao, M.-Q.; Yang, J.; Giammarco, J. M.; Qiu, J.; Barsoum, M. W.; Gogotsi, Y. Flexible and conductive MXene films and nanocomposites with high capacitance. *Proc. Natl. Acad. Sci. U.S.A.* **2014**, *111*, 16676−16681.

DOI: 10.1021/acsomega.8b02032
ACS Omega 2018, 3, 12489−12494